SCYL1BP1 modulates neurite outgrowth and regeneration by regulating the Mdm2/p53 pathway

Yonghua Liu[a,b,*], Ying Chen[b,*], Xiang Lu[b], Youhua Wang[b], Yinong Duan[b], Chun Cheng[b,*], and Aiguo Shen[a]

[a]Jiangsu Province Key Laboratory of Neuroregeneration, Nantong University, Nantong 226001, China; [b]Department of Pathogen Biology, Medical College, Nantong University, Nantong 226001, China

ABSTRACT **SCY1-like 1–binding protein 1 (SCYL1BP1) is a newly identified transcriptional activator domain containing a protein with many unknown biological functions. Recently emerging evidence has revealed that it is a novel regulator of the p53 pathway, which is required for neurite outgrowth and regeneration. Here we present evidence that SCYL1BP1 inhibits nerve growth factor–mediated neurite outgrowth in PC12 cells and affects morphogenesis of primary cortical neurons by strongly decreasing the p53 protein level in vitro, all of which depends on SCYL1BP1's transcriptional activator domain. Exogenous p53 rescues neurite outgrowth and neuronal morphogenesis defects caused by SCYL1BP1. Furthermore, SCYL1BP1 can directly induce Mdm2 transcription, whereas inhibiting the function of Mdm2 by specific small interfering RNAs results in partial rescue of neurite outgrowth and neuronal morphogenesis defects induced by SCYL1BP1. In vivo experiments show that SCYL1BP1 can also depress axonal regeneration, whereas inhibiting the function of SCYL1BP1 by specific short hairpin RNA enhances it. Taken together, these data strongly suggested that SCYL1BP1 is a novel transcriptional activator in neurite outgrowth by directly modulating the Mdm2/p53-dependent pathway, which might play an important role in CNS development and axonal regeneration after injury.**

Monitoring Editor
William P. Tansey
Vanderbilt University

Received: May 14, 2012
Revised: Oct 2, 2012
Accepted: Oct 5, 2012

INTRODUCTION

Neurite outgrowth, sprouting, and regeneration require an orchestrated sequence of events. There is compelling evidence that the tumor suppressor protein p53 regulates neurite outgrowth and regeneration in vitro and in vivo. As a transcription factor, p53 is required for nerve growth factor (NGF)–mediated differentiation of PC12 cells via regulation of high-affinity NGF receptor TrkA levels (Zhang *et al.*, 2006). p53 is also required for neurite outgrowth in cultured cells, including primary neurons and PC12 cells, as well as for axonal regeneration in vivo in mice via increased expression of coronin 1b (a filamentous actin–binding protein), the small GTPase Rab13 (Di Giovanni *et al.*, 2006), and the cGMP-dependent protein kinase type I (Tedeschi *et al.*, 2009b). In addition, p53 plays a direct role in axon outgrowth by occupying the promoter of the proaxon growth gene GAP-43 (Tedeschi *et al.*, 2009a). In addition to its transcriptional function, p53 plays a novel role in axonal growth cone behavior, acting as a suppressor of ROCK activity (Qin *et al.*, 2009). These results suggest that p53 regulates neurite outgrowth and regeneration in both transactivation-dependent and transactivation-independent manners. Nonetheless, few endogenous cellular pathway molecules have been reported to be involved in the regulation of neurite outgrowth through a transcriptional activity or a nontranscriptional effect of p53, such as dysbindin-1 (Ma *et al.*, 2011) and calpain (Qin *et al.*, 2010), respectively.

This article was published online ahead of print in MBoC in Press (http://www.molbiolcell.org/cgi/doi/10.1091/mbc.E12-05-0362) on October 10, 2012.

*These authors contributed equally to this work.

Address correspondence to: Aiguo Shen (shen_aiguo@yahoo.com).

Abbreviations used: BRCT, breast carboxy-terminal; cGKI, cGMP-dependent protein kinase type I; ChIP, chromatin immunoprecipitation; DIV, days in vitro; F-actin, filamentous actin; GAP-43, growth-associated protein 43; mdm2, murine double minute 2; NGF, nerve growth factor; PML, promyelocytic leukemia; pRb, retinoblastoma protein; SCYL1BP1, SCY1-like 1 binding protein 1; UPS, ubiquitin-proteasome system; YY1, Yin Yang 1.

p53 is a protein with a short half-life and is maintained at low or undetectable levels by continual proteolytic degradation in normal cells. Sustained degradation of p53 is mediated by the ubiquitin-proteasome system (Maki *et al.*, 1996), mainly by the E3 ligase Mdm2 (Fuchs *et al.*, 1998; Fang *et al.*, 2000). By binding p53, Mdm2 also conceals the transactivation domain of p53 and therefore inhibits its transcriptional activity (Kubbutat and Vousden, 1998). In addition, Mdm2 is required to promote p53 nuclear export and subsequently decrease its transcriptional activity (Boyd *et al.*, 2000; Geyer *et al.*, 2000). Mdm2 itself is also a transcriptional target of p53 (Kubbutat and Vousden, 1998; Prives, 1998). These data reveal a feedback loop that regulates both p53 activity and the expression of Mdm2, which is critical for maintaining normal cellular physiology. Challenged with stress signals such as hypoxia or DNA damage, the feedback loop of Mdm2-p53 is disturbed, leading to apoptosis or malignancy (Marine *et al.*, 2006). However, little is known about the role of the Mdm2–p53 feedback loop in neurite outgrowth and regeneration.

Several factors have been described to affect the feedback loop of Mdm2–p53, such as retinoblastoma protein, transcriptional factor Yin Yang 1, promyelocytic leukemia (Bernardi *et al.*, 2004), and SCY1-like 1–binding protein 1 (SCYL1BP1). SCYL1BP1 is a newly identified regulator of the Mdm2–p53 feedback loop, which directly binds to Mdm2 and promotes Mdm2 self-ubiquitination, subsequently stabilizing p53 (Yan *et al.*, 2010a,b). SCYL1BP1, initially identified as an SCYL1-binding protein (Di *et al.*, 2003), is an evolutionally conserved protein existing in different organisms ranging from plants to animals. SCYL1BP1 protein is observed in many normal tissues and is mainly localized in the cytoplasm, with a low level in the nucleus. Bioinformatics analysis reveals that SCYL1BP1 protein has a predicted bipartite nuclear localization signal, a breast carboxy-terminal domain, two coiled-coil domains, and a transcriptional activator domain (Di *et al.*, 2003). All these results strongly suggest that SCYL1BP1 might play an important role in transcriptional activity. Therefore we hypothesized that SCYL1BP1 regulated the Mdm2–p53 feedback loop not only via proteins interactions, but also through unknown transcriptional mechanisms.

In the present study, we characterize the function of SCYL1BP1 in neurite outgrowth and regeneration. Overexpression of SCYL1BP1 inhibits NGF-mediated neurite outgrowth of PC12 cells and affects morphogenesis of cortical neurons via transcriptional regulating Mdm2 expression and consequently p53 inhibition. In addition, overexpression of SCYL1BP1 inhibits neuronal regeneration after facial nerve axotomy, whereas inhibiting the function of SCYL1BP1 by specific short hairpin RNA (shRNA) enhances it. Our data delineate a novel SCYL1BP1–Mdm2–p53 axis that contributes to the regulation of neurite outgrowth and regeneration.

RESULTS

Exogenous SCYL1BP1 attenuates NGF-mediated neurite outgrowth of PC12 cells and affects the morphogenesis of cortical neurons

To investigate the role of SCYL1BP1 in axon outgrowth, we first examined expression patterns of SCYL1BP1 during NGF-mediated neurite outgrowth of PC12 cells and morphogenesis of primary cortical neurons cultured in vitro. Western blot showed that SCYL1BP1 expression was decreased at different times after 100 ng/ml NGF treatment in naive PC12 cells, which was similar to the dynamics we observed in primary neurons prepared from E18 rat cortex and cultured for different days in vitro (DIV; Figure 1, A and B). Alternatively, immunofluorescence staining was performed to identify the distribution of endogenous SCYL1BP1. In naive PC12 cells, SCYL1BP1 had a high level in the cytoplasm and a low level in the nuclei. After NGF treatment, SCYL1BP1 expression was largely decreased in both components, especially in nuclei (Figure 1C). Similar dynamics was observed in primary cortical neurons (Figure 1D). Furthermore, cell fractionation assays were performed and showed identical results (Figure 1, E and F). We then hypothesized that SCYL1BP1 could be important for neuronal morphogenesis.

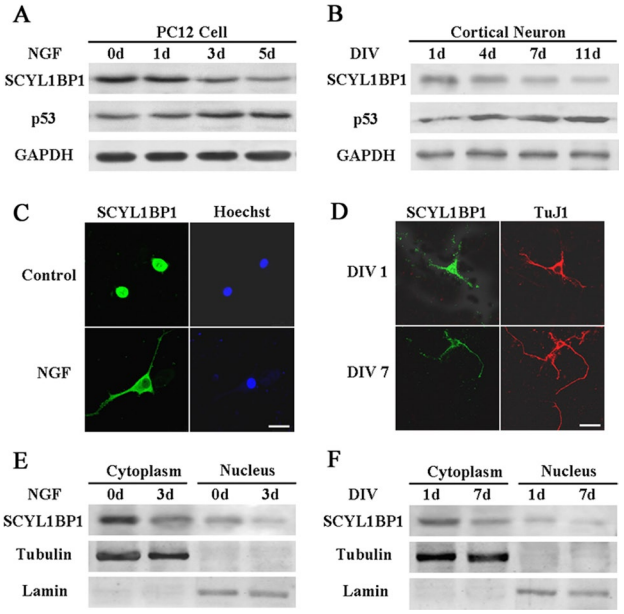

FIGURE 1: Endogenous SCYL1BP1 expression in naive PC12 cells and primary cortical neurons. (A) Western blot analysis of SCYL1BP1 and p53 expression in PC12 cells 0, 1, 3, and 5 d after 100 ng/ml NGF treatment. Glyceraldehyde-3-phosphate dehydrogenase (GAPDH) was used as a loading control. (B) Western blot analysis of SCYL1BP1 and p53 expression in cultured cortical neurons at DIV 1, 4, 7, and 11. (C, D) Immunofluorescence staining was performed to identify the distribution of endogenous SCYL1BP1 in naive PC12 cells and primary neurons, respectively. Hoechst 33342–stained nuclei and TuJ1-stained neurons. Scale bar, 50 μm. (E, F) Cell fractionation assays were performed in naive PC12 cells and primary cortical neurons, respectively. The levels of α-tubulin and lamin B in the nuclear and cytosolic fractions, respectively, were immunoblotted to confirm the purity of the subcellular fractions.

To test our hypothesis, we generated a naive PC12 cell line that stably expresses SCYL1BP1 and examined cell morphology by phase-contrast microscopy. We found that NGF treatment could induce PC12 cells to undergo differentiation, which was blocked by the overexpression of SCYL1BP1 (Figure 2B). To confirm this observation, we quantified neurite outgrowth. The percentage of cells with neurites longer than two body lengths was calculated, and at least 500 cells were assayed in each group. The percentage of cells with neurites longer than two body lengths was conspicuously decreased by SCYL1BP1, ranging from 15% to 4.5% (Figure 2C). To further investigate the role of SCYL1BP1 in axon outgrowth, we generated two mutants of SCYL1BP1: BP1-N, which lacks the transcriptional activator region, and BP1-T, which contains the C-terminal transcriptional activator region (Figure 2A). Like SCYL1BP1, BP1-T also attenuates NGF-mediated neurite outgrowth of PC12 cells (Figure 2, B and C). Because SCYL1BP1 impaired neurite outgrowth, MTT assays were performed to examine whether it affected cell viability; both SCYL1BP1 and BP1-T, but not BP1-N, increased PC12 cell viability (Supplemental Figure S1A). A

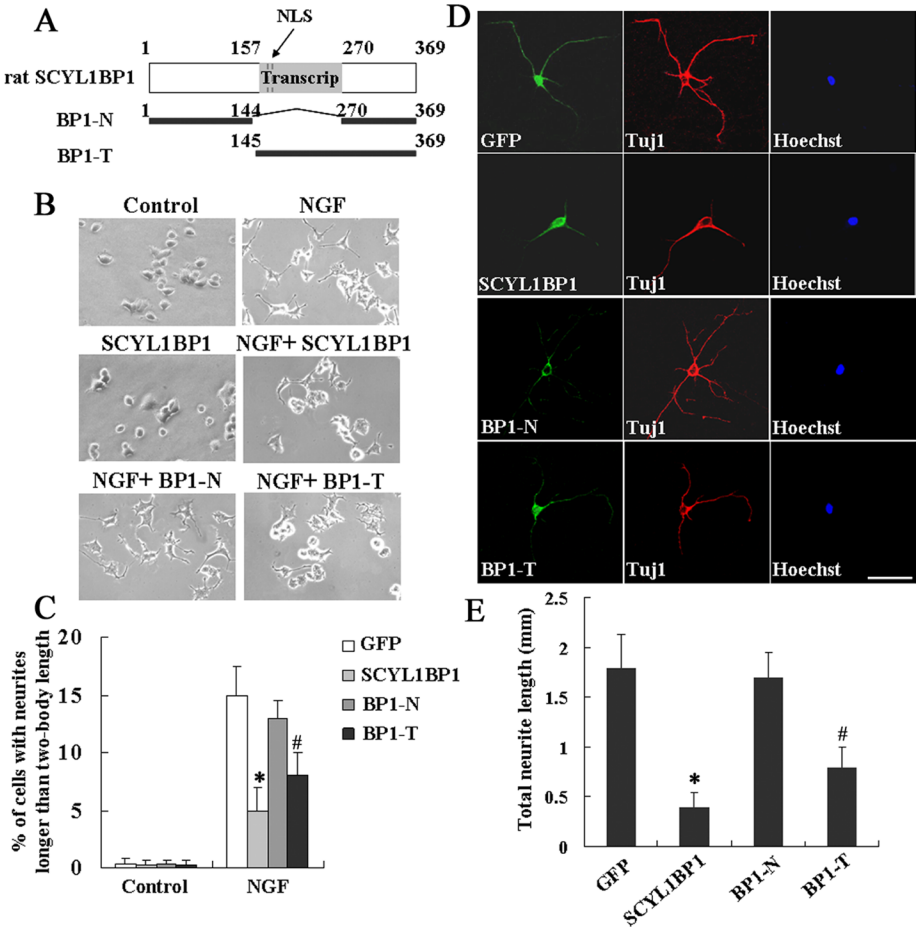

FIGURE 2: SCYL1BP1 regulates neurite outgrowth and neuronal morphogenesis in vitro. (A) Schematic structure of SCYL1BP1, BP1-N, and BP1-T. NLS, nuclear localization signal; Transcrip, transcriptional activator domain. (B) Representative microscopy images of PC12 cells with or without SCYL1BP1, BP1-N, or BP1-T expression in the presence or absence of NGF for 3 d. (C) Quantitative analysis of PC12 cells bearing neurites as shown in B. The percentage of cells with neurites longer than two body lengths was calculated. At least 500 cells were counted for each treatment, and the error bars represent the SD of triplicate results. (D) Representative images of neurons transfected with GFP, SCYL1BP1, BP1-N, or BP1-T. TuJ1-stained neurons. Scale bar, 100 μm. (E) Quantitative analysis of total neurite length of neurons treated as in D. Data represent mean ± SEM; $n = 50–70$ in each group; $^{*,\#}p < 0.01$; *t* test.

SCYL1BP1 knockdown experiment was also performed with lentivirus encoding green fluorescent protein (GFP) or together with SCYL1BP1 shRNA. SCYL1BP1 shRNA 1 resulted in ~80% reduction in SCYL1BP1 level when compared with control shRNA (Supplemental Figure S1B). SCYL1BP1 shRNA 1 did not affect naive PC12 cell neurite outgrowth without NGF, whereas after NGF treatment, SCYL1BP1 shRNA 1 enhanced neurite outgrowth of PC12 cells (Supplemental Figure S1, C and D).

In addition, we transfected cultured cortical neurons with lentivirus encoding GFP or together with SCYL1BP1, BP1-N, or BP1-T soon after plating and analyzed neuronal morphology at DIV 4. Infection of primary cortical neurons with lentiviral particles carrying the SCYL1BP1 or BP1-T plasmid resulted in a marked reduction in the total length of both dendrites and axons (Figure 2, D and E), which suggested that overexpression of SCYL1BP1 in cortical neurons could inhibit neuronal morphogenesis. Taken together, these data suggest that SCYL1BP1, with its transcriptional activator domain, serves as a potent suppressor of neuronal morphogenesis in vitro.

p53 antagonizes the effect of SCYL1BP1 on neurite outgrowth and neuronal morphogenesis

Previous studies showed that there was an inevitable link between SCYL1BP1 and the p53 pathway (Yan *et al.*, 2010a). In addition, p53 was also found to be required for axon outgrowth (Di Giovanni *et al.*, 2006; Zhang *et al.*, 2006; Tedeschi *et al.*, 2009a). Accordingly, we probed the possibility that SCYL1BP1 affects neuronal morphogenesis by targeting p53. Lysates from NGF-treated PC12 cells and cultured primary cortical neurons exhibited increased p53 expression over time, contrary to the kinetics of SCYL1BP1 expression (Figure 1, A and B), suggesting that SCYL1BP1 could serve as a potential regulator of p53 during axon outgrowth and neuronal morphogenesis. To further address this possibility, we examined mRNA and protein levels of p53 in PC12 and primary cortical neurons infected with SCYL1BP1. To our surprise, overexpression of SCYL1BP1 or BP1-T significantly reduced the expression of p53 on protein levels, but not on mRNA levels, in both PC12 cells and cultured cortical neurons (Figure 3, A and B). This is quite different from a recent report, in which an increase in SCYL1BP1 protein levels caused a surge in the amount of p53 protein (Yan *et al.*, 2010a). Down-regulation of p53 by SCYL1BP1 was attenuated when cells were treated with the 26S proteasome inhibitor MG132 (Supplemental Figure S2A), suggesting that the regulation of p53 by SCYL1BP1 was probably accomplished by accelerating protein turnover. To further verify this possibility, we analyzed the half-life of p53 protein. PC12 cells were treated with cycloheximide for 0.5–8 h to prevent further protein synthesis. As shown in Supplemental Figure S2B, the half-life of p53 protein was clearly reduced by ectopically expressed SCYL1BP1. All these results suggest that SCYL1BP1, with its transcriptional activator domain, may decrease p53 protein level by promoting its degradation in neuronal cells.

Next we examined the effect of p53 on SCYL1BP1-mediated inhibition of neurite outgrowth and neuronal morphogenesis. In NGF-treated PC12 cells, neurite outgrowth defect induced by SCYL1BP1 was largely prevented by cotransfecting p53 (Figure 3, C and D). p53 alone promoted neurite outgrowth in PC12 cells, as evidenced by extensive and longer neurites, which was consistent with a previous report (Zhang *et al.*, 2006). Similar observations were made in primary cortical neurons (Figure 3, E and F). Thus we conclude that inhibition of neurite outgrowth and neuronal morphogenesis by SCYL1BP1 may result from destabilization of p53.

Mdm2 knockdown rescues neurite outgrowth and neuronal morphogenesis defects caused by SCYL1BP1

Next we examined the mechanism by which SCYL1BP1 promotes p53 degradation. Mdm2 and Pirh2, both of which can bind to SCYL1BP1 directly, are the two major E3 ligases involved in p53

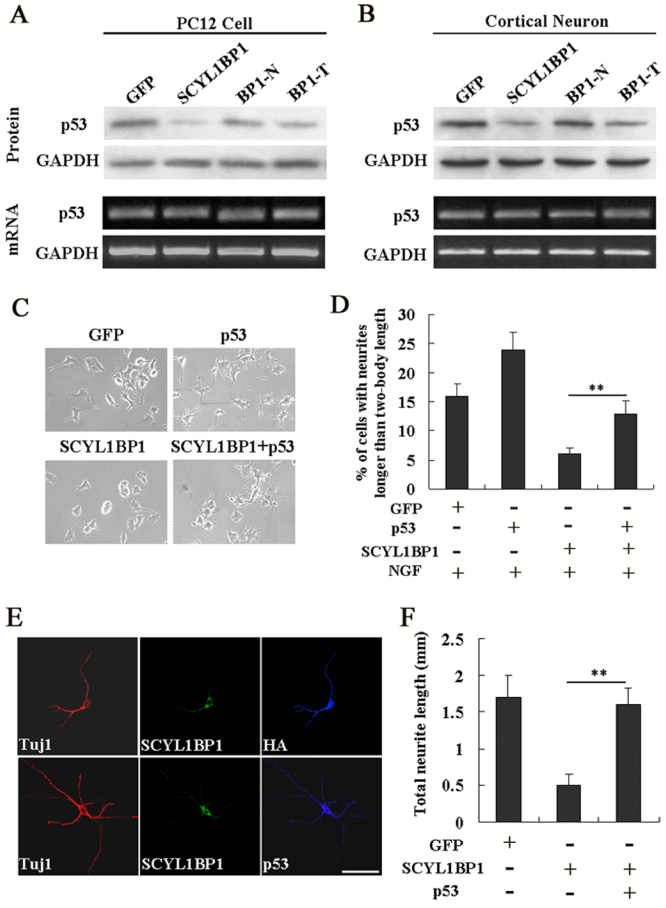

FIGURE 3: p53 rescues neurite outgrowth and neuronal morphogenesis defects caused by SCYL1BP1. (A, B) Western blot and RT-PCR analysis of p53 expression in PC12 cells (A) and cultured cortical neurons (B) after overexpression of SCYL1BP1, BP1-N, or BP1-T. (C) Representative microscopy images of PC12 cells with indicated constructs after 100 ng/ml NGF treatment for 3 d. (D) Quantitative analysis of PC12 cells bearing neurites as shown in C. (E) Representative images of neurons transfected with SCYL1BP1 together with HA or p53. Scale bar, 100 μm. (F) Quantitative analysis of total dendritic length of neurons treated as in E. Data represent mean ± SEM; $n = 50–70$ in each group; $^{**}p < 0.01$; *t* test.

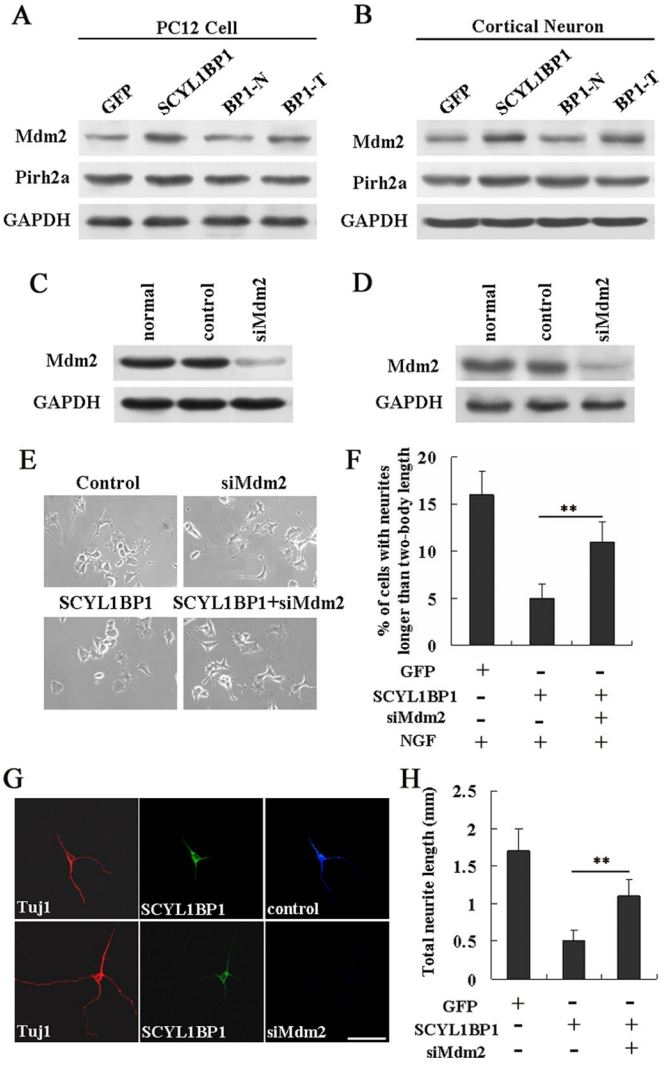

FIGURE 4: Mdm2 knockdown rescues neurite outgrowth and neuronal morphogenesis defects caused by SCYL1BP1. (A, B) Western blot analysis of Mdm2 and Pirh2 expression in PC12 cells (A) and cultured cortical neurons (B) after overexpression of SCYL1BP1, BP1-N, or BP1-T. (C, D) Down-regulation of Mdm2 in PC12 cells (C) and cultured cortical neurons (D) by siRNA. (E) Representative microscopy images of PC12 cells with indicated constructs in the presence of NGF for 3 d. (F) Quantitative analysis of PC12 cells bearing neurites as shown in E. (G) Representative images of neurons transfected with SCYL1BP1 together with control or siMdm2. Scale bar, 100 μm. (H) Quantitative analysis of total dendritic length of neurons treated as in G. Data represent mean ± SEM; $n = 50–70$ in each group; $^{**}p < 0.01$; *t* test.

degradation (Leng *et al.*, 2003; Logan *et al.*, 2004; Zhang *et al.*, 2005; Duan *et al.*, 2006; Yan *et al.*, 2010a). We hypothesized that SCYL1BP1 might destabilize p53 protein by up-regulating Pirh2 and/or Mdm2. This hypothesis was first tested in both PC12 cells and cultured cortical neurons. Immunoblotting assays showed that overexpression of SCYL1BP1 or BP1-T up-regulated the expression of Mdm2 but not Pirh2 (Figure 4, A and B). Then we examined the role of Mdm2 knockdown on SCYL1BP1-induced neurite outgrowth and neuronal morphogenesis defects. siMdm2 resulted in ~70% reduction in Mdm2 level when compared with control siRNA (Figure 4, C and D). In NGF-treated PC12 cells, neurite outgrowth defects induced by SCYL1BP1 were partly prevented by Mdm2 knockdown (Figure 4, E and F). Similar results were obtained in primary cortical neurons (Figure 4, G and H). Taken together, these results demonstrate that SCYL1BP1, with its transcriptional activator domain, antagonizes p53-induced neurite outgrowth and neuronal morphogenesis by up-regulating the expression Mdm2.

SCYL1BP1 attenuates neurite outgrowth and morphogenesis by inducing Mdm2 transcription

To further investigate how SCYL1BP1 up-regulates Mdm2, we examined Mdm2 expression at both the mRNA and protein levels. Reverse transcription (RT)-PCR assays showed that overexpression of SCYL1BP1 or BP1-T significantly up-regulated the Mdm2 mRNA level in both PC12 cells and cultured cortical neurons (Figure 5, A and B). The half-life of Mdm2 was not notably altered with or without SCYL1BP1 overexpression (Figure 5C). These data suggest that SCYL1BP1 probably up-regulates Mdm2 expression mainly at the transcriptional level. To directly test whether SCYL1BP1 induces Mdm2 transcription rate, we amplified a fragment spanning Mdm2

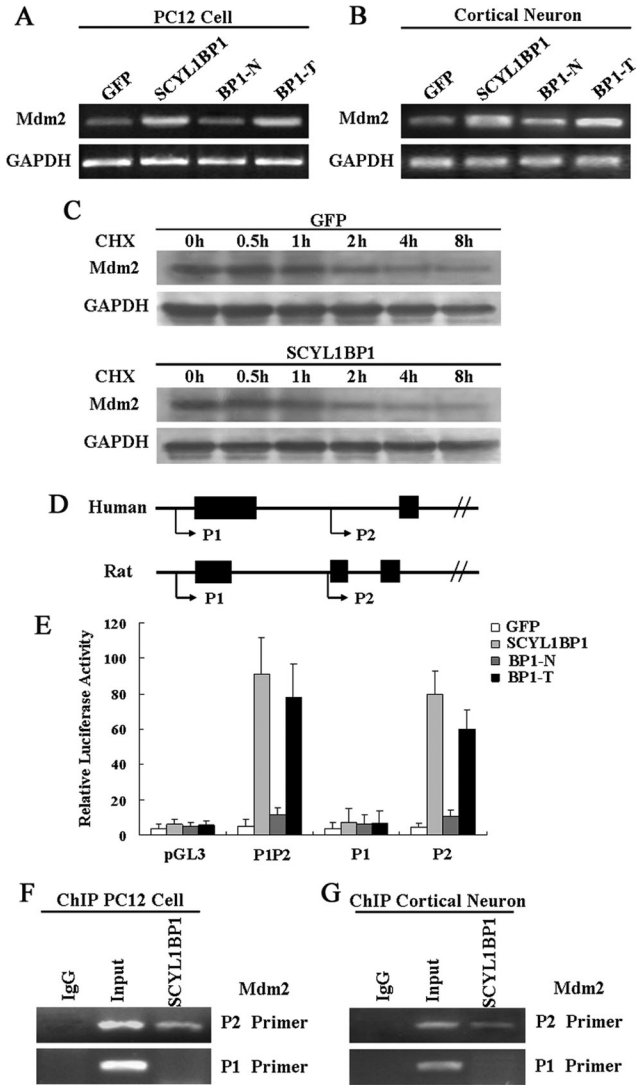

FIGURE 5: SCYL1BP1 induces Mdm2 transcription. (A, B) RT-PCR analysis of Mdm2 expressions in PC12 cells (A) and cultured cortical neurons (B) after overexpression of SCYL1BP1, BP1-N, or BP1-T. (C) SCYL1-BP1 did not change the half-life of Mdm2. PC12 cells were transfected with or without SCYL1-BP1. At 48 h posttransfection, the cells were treated with 50 μg/ml CHX for the indicated times. Lysates were prepared and analyzed by Western blotting for Mdm2 and the GAPDH loading control. (D) Schematic diagrams showing human and rat genomic DNA structures of *Mdm2* with two distinct promoters designated P1 and P2. In human, P1 is a constitutive promoter, and P2 is a p53-responsive promoter that is located between exons 1 and 2 of the gene. An identical length is designated for rat. (E) Dual luciferase assay was performed as described in *Materials and Methods*. PC12 cells were transfected with a Mdm2 luciferase reporter derived from P1P2, P1, or P2 and plasmids expressing GFP, SCYL1-BP1, BP1-N, or BP1-T, as indicated, and luciferase activity was assayed. The results were normalized to *Renilla* luciferase activity and represent the mean ± SD of three independent experiments. (F, G) ChIP assays were performed in PC12 cells (F) and cultured cortical neurons (G) as described in *Materials and Methods*. Rabbit anti–SCYL1-BP1 antibody was used to immunoprecipitate SCYL1-BP1–DNA complexes. Rabbit immunoglobulin G was used as a control.

promoter from nucleotide (nt) –1513 to +287 relative to the transcription start site from the rat genome using PCR. In accord with the human Mdm2 promoter, the rat Mdm2 promoter was also designated as two distinct promoters, P1 and P2. P1 promoter, which is from nt –1513 to –513, contains exon 1. P2 promoter, which is from nt –512 to +287, contains exons 2 and 3. The total promoter from nt –1513 to +287 was designated as P1P2. Then all of them were cloned for luciferase assay (Figure 5D). We showed that P1P2 promoter led to a noticeable increase of luciferase activity by SCYL1BP1 or BP1-T, and P2 promoter led to a similar level, whereas P1 promoter led to a slight increase (Figure 5E). These results suggested that SCYL1BP1, with its transcriptional activator domain, could directly induce Mdm2 promoter, in which P2 promoter but not P1 promoter was required.

To demonstrate that SCYL1BP1 can directly bind to the Mdm2 promoter, we performed chromatin immunoprecipitation (ChIP) with primers to amplify fragments in both P1 and P2 promoters. Indeed, P2 promoter was immunoprecipitated by SCYL1BP1 in both PC12 cells and cultured cortical neurons, but P1 promoter was not (Figure 5, F and G). Subsequently we asked how SCYL1BP1 interacted with the P2 promoter of the *Mdm2* gene during neurite outgrowth of both PC12 cells and primary cortical neurons. ChIP assays showed that their interaction decreased over time after NGF treatment in PC12 cells; an identical result was observed in cultured 1–11-DIV neurons (Supplemental Figure S3).

Exogenous SCYL1BP1 attenuates physiological nerve regeneration

The in vitro data suggest that SCYL1BP1 inhibits NGF-induced, p53-dependent neurite outgrowth of PC12 cells and morphogenesis of cortical neurons. We next asked whether SCYL1BP1 could play a role in axonal regeneration in vivo. To this end, we compared the extent of nerve regeneration in rats injected with lentivirus encoding GFP or SCYL1BP1 or saline into facial nuclei after facial nerve axotomy, an established model for regeneration (Raivich *et al.*, 2004). The extent of regeneration was assessed by counting fluorescent motor neurons in the facial motor nuclei with the retrograde nerve tracer FluoroGold at 21 d after facial nerve injury. It is striking that there was a significant decrease in the number of regenerating fibers in SCYL1BP1-injected animals as compared with saline or GFP animals (Figure 6A). The percentage of FluoroGold-positive neurons was 28.8 ± 4.5% and 26 ± 3.5%, respectively, in the saline and GFP animals versus 11.77 ± 1.6% in the SCYL1BP1-injected animals (Figure 6, B and C); this difference was highly significant (*t* test, $p < 0.01$). To examine the toxic effects of lentivirus encoding GFP or together with SCYL1BP1, we measured the survival and DNA integrity of facial nuclei. Both showed slight toxic effects, as a single terminal deoxynucleotidyl transferase dUTP nick end labeling–positive cell was observed (Supplemental Figure S4). To further investigate the role of SCYL1BP1 in nerve regeneration, we also used lentivirus encoding SCYL1BP1 shRNA. As expected, SCYL1BP1 knockdown enhanced axonal regeneration (Figure 6, D and E).

DISCUSSION

Complex neuronal morphology forms the basis of proper neuronal connectivity and brain function. Establishment of neuronal morphology during development is a highly regulated process, with sprouting and elongation of neurites, later developing into axons and dendrites. This multistep process is regulated by both intrinsic genetic programs and external signals (Whitford *et al.*, 2002; Miller and Kaplan, 2003).

SCYL1BP1 was initially identified as an SCYL1-binding protein (Di *et al.*, 2003), but little is known about its biological function. Recent work showed that loss-of-function mutations of *SCYL1BP1* caused gerodermia osteodysplastica (Hennies *et al.*, 2008), which

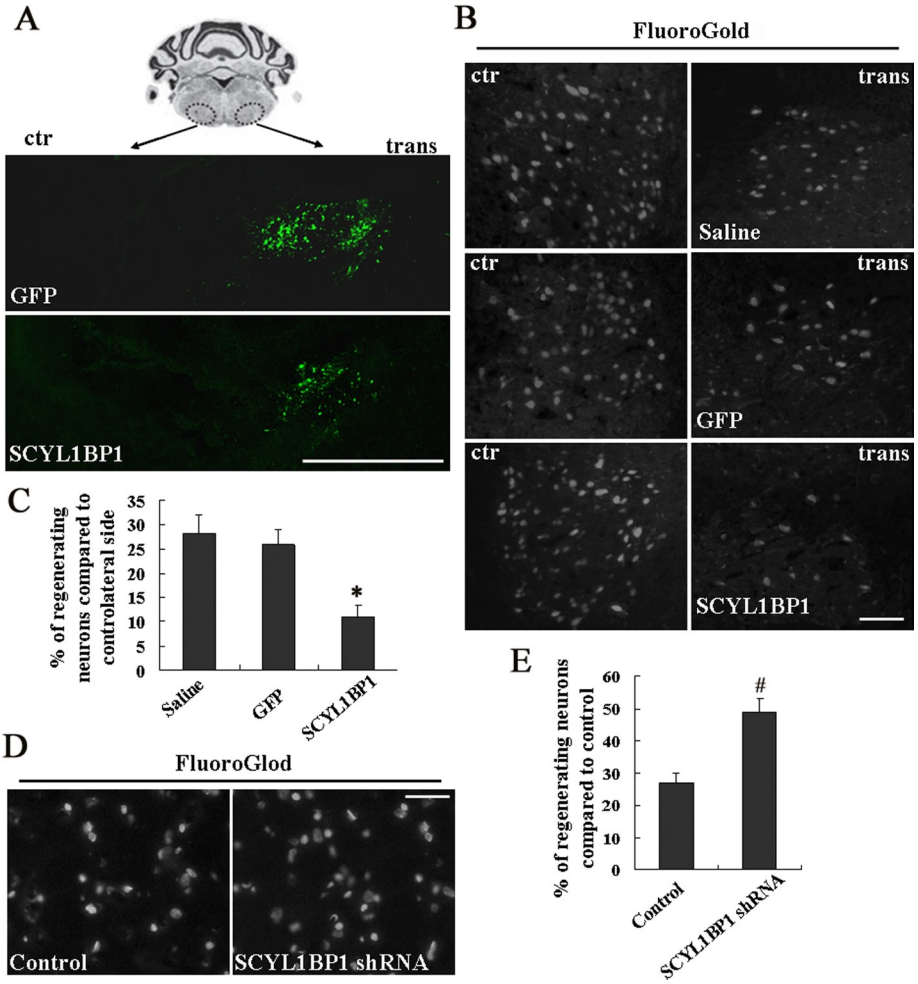

FIGURE 6: SCYL1BP1 modulates physiological nerve regeneration. (A) Lentivirus encoding GFP or together with SCYL1BP1 were injected into facial nuclei after facial nerve axotomy, an established model for regeneration. Scale bar, 500 μm. (B) The extent of regeneration was assessed by counting fluorescent motor neurons in the facial motor nuclei with the retrograde nerve tracer FluoroGold 21 d after injury. Scale bar, 20 μm. (C) Bar graphs show quantitation of regenerating facial motor neurons 21 d after facial transection. The percentage of FluoroGold-positive neurons was 28.8 ± 4.5% and 26 ± 3.5%, respectively, in the saline and GFP animals vs. 11.77 ± 1.6% in the SCYL1BP1-injected animals. (five animals per group; *unpaired two-tailed *t* test with $p < 0.01$). (D) The extent of regeneration was assessed by counting fluorescent motor neurons in the facial motor nuclei with the retrograde nerve tracer FluoroGold 21 d after injury. Scale bar, 20 μm. (E) Bar graphs show quantitation of regenerating facial motor neurons 21 d after facial transection. The percentage of FluoroGold-positive neurons was 27.3 ± 3.5% in control animals vs. 49.77 ± 4.2% in SCYL1BP1 shRNA–injected animals (five animals per group, #unpaired two-tailed *t* test $p < 0.01$).

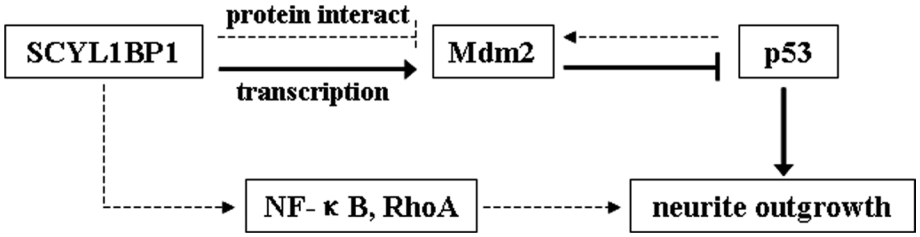

FIGURE 7: Model of SCYL1BP1 regulation and action in neurite outgrowth. SCYL1BP1 binds to *Mdm2* promoter and enhances its transcription. Mdm2 inhibits p53 activity. p53 is also required for neurite outgrowth. Whether the role of SCYL1BP1 in neurite outgrowth suppression depends on transcriptional regulation of the NF-κB and/or RhoA pathway needs further investigation. Solid lines, the data from our present work. Dotted lines, the data from previous reports or our hypothesis.

suggested that *SCYL1BP1* is an important pathogenic candidate gene. More recently, SCYL1BP1 was identified as a new regulator of the p53 pathway (Yan *et al.*, 2010a). So it is perhaps not surprising that SCYL1BP1 has broader roles in physiology and pathology, such as the regulation of stress, metabolism, autophagy, tumors, and development. Here our specific aim is to investigate the potential roles of SCYL1BP1 in the regulation of neurite outgrowth and regeneration.

We first found that SCYL1BP1 decreased during NGF-mediated neurite outgrowth of PC12 cells and morphogenesis of cortical neurons cultured in vitro. Concomitantly, p53 protein increased. SCYL1BP1 or BP1-T overexpression attenuates NGF-mediated neurite outgrowth of PC12 cells and morphogenesis of cortical neurons by p53 inhibition. Furthermore, neurite outgrowth and neuronal morphogenesis defects induced by SCYL1BP1 are largely prevented by cotransfecting p53. In addition, SCYL1BP1 or BP1-T can directly induce Mdm2 transcription, and inhibition of Mdm2 function by specific siRNAs results in partial rescue of neurite outgrowth and neuronal morphogenesis defects induced by SCYL1BP1. Additional experiments showed that SCYL1BP1 also decreases axonal regeneration in vivo, whereas inhibiting the function of SCYL1BP1 by specific shRNA enhances it. Taken together, these data strongly support the existence of an unexpected and critical function of SCYL1BP1 in neurite outgrowth, which could play important roles during CNS development and in axonal regeneration after injury.

Bioinformatics analysis reveals that SCYL1BP1 protein has a predicted bipartite nuclear localization signal and a transcriptional activator domain (Di *et al.*, 2003). These data strongly suggest that SCYL1BP1 may play an important transcriptional activating role. In the present study, we found that SCYL1BP1 bound to *Mdm2* promoter and enhanced its transcription. Subsequently ChIP–quantitative PCR assays showed that SCYL1BP1 also bound to the promoters of NF-κB, interleukin 6, and RhoA, besides Mdm2 (Li, 2010). These data imply that SCYL1BP1 did play a role as a novel transcriptional activator.

Previous data showed that SCYL1BP1 could directly bind to Mdm2 and promote Mdm2 self-ubiquitination (Yan *et al.*, 2010b). Therefore we hypothesize that there is a new regulating loop between SCYL1BP1 and Mdm2, in which SCYL1BP1 up-regulates Mdm2 at the transcriptional level and down-regulates it at posttranscriptional level (Figure 7). In addition to p53, NF-κB and

RhoA were also reported to play important roles in neural process growth, elaboration, and structural plasticity (Koh, 2006–2007; Boersma *et al.*, 2011; Gutierrez and Davies, 2011). Accordingly, we conclude that SCYL1BP1 binds to *Mdm2* promoter and enhances its transcription, ultimately inhibiting p53 activity and suppressing neurite outgrowth. Whether the role of SCYL1BP1 in neurite outgrowth suppression depends on transcriptional regulation of the NF-κB and/or RhoA pathway needs further investigation (Figure 7).

In conclusion, our work provides strong evidence for a novel role of SCYL1BP1 in neurite outgrowth and nerve regeneration and provides the molecular framework for such a function. Modulation of this SCYL1BP1/Mdm2/p53-dependent pathway may provide a novel therapeutic target for facilitating neuroplasticity and neuroregeneration after injuries to the central or peripheral nervous system.

MATERIALS AND METHODS

Expression plasmid preparation

To obtain full-length rat *SCYL1BP1*, 5′-end primer (5′-CGC TCG AGG TAT GGC TCA GGG TTG GGC TG-3′) and 3′-end primer (5′-AGG GTA CCC GTG GCC ACA GCG GCT GGA AAG-3′) were designed to amplify a cDNA library of rat cortex by PCR. The PCR products were cloned into pEGFP-N3 at *Xho*I and *Kpn*I sites. An identical method was used for BP1-N, BP1-T, and hemagglutinin (HA)-tagged rat p53. To generate the luciferase reporter under the control of the *Mdm2* promoter (P1P2), a 1800–base pair DNA fragment containing the *Mdm2* promoter was amplified from genomic DNA purified from PC12 cells using an upstream primer, 5′-TTG AGC TCT TAG GTC CCC TGG AAT GAC AG-3′, and a downstream primer, 5′-ATC TCG AGT GCC TTT CTA AAG CCA GCG TC-3′. The DNA fragment was then cloned into pGL3-basic vector at *Sac*I and *Xho*I sites. To generate the luciferase reporters P1 and P2, a *Sac*I and *Xho*I fragment obtained from the P1P2 was cloned into pGL3-Basic (Promega, Madison, WI). All constructs were verified by sequencing.

Small interfering RNAs and transfection

Mdm2 small interfering RNA (siRNA) was purchased from Santa Cruz Biotechnology (Santa Cruz, CA; sc-63266). Briefly, the siRNA product generally consists of pools of three to five target-specific 19- to 25-nt siRNAs designed to knock down Mdm2 expression. Transfection was performed according to manufacturer's instructions.

Recombinant lentiviral vector packaging and infection

To get SCYL1BP1-overexpressing lentivirus, full-length SCYL1BP1 was cloned into the pLenti6/entre plasmid (Invitrogen, Carlsbad, CA) according to manufacturer's instructions. A 3-μg amount of pLenti6/entre-SCYL1BP1-EGFP vector and 9 μg of ViraPower Packaging Mix (Invitrogen) were used to cotransfect 5×10^6 HEK293T cells with Lipofectamine 2000. At 48 h after transfection, the supernatant containing the viruses (Lenti-EGFP-SCYL1BP1) was harvested, centrifuged, and stored at −80°C. Lentiviruses were titrated using HEK293 cells with serial dilutions of virus stocks, followed by fluorescence microscopy examination 3 d after infection at $(2–3) \times 10^9$ infectious units/ml.

Reagents and antibodies

The following reagents and antibodies were used in this study: rabbit polyclonal anti-SCYL1BP1 (ab68452; Abcam, Cambridge, MA), mouse monoclonal anti-p53 (sc-6243; Santa Cruz Biotechnology), mouse monoclonal anti-TuJ1(MAB1637; Millipore, Billerica, MA), goat polyclonal anti-Mdm2 (ab3110; Abcam), rabbit polyclonal anti-Pirh2a (SAB2101970; Sigma-Aldrich, St. Louis, MO), rabbit polyclonal anti-GAPDH (ab9484; Abcam), and goat polyclonal anti-HA (ab9134; Abcam). Z-Leu-Leu-Leu-al (MG132) and cycloheximide (CHX) were purchased from Sigma-Aldrich. The dual-luciferase assay kit and NGF (murine, 2.5 s) were purchased from Promega.

Cell culture and transfection

The PC12 cells were maintained in Ham's F12 medium supplemented with 15% horse serum and 2.5% fetal bovine serum (Invitrogen). For generation of the SCYL1BP1 stably expressing cell line, parental PC12 cells were transfected with a pEGFP-N3 vector, which expresses the neomycin-resistant gene for clone selection. Cells were selected with 500 mg/ml G418 (4727878001; Roche, Indianapolis, IN) for 4 wk. Individual clones were screened for stable expression of SCYL1BP1 by immunofluorescence analyses and Western blot analysis.

Cortical and hippocampal neurons were dissociated from embryonic day 18 (E18) Sprague Dawley rat embryos. Briefly, cortices were minced and dissociated in the same buffer with 1800 U/ml trypsin at 37°C for 20 min. After the addition of 200 U/ml DNase I and 3600 U/ml soybean trypsin inhibitor to the suspension, cells were triturated through a 5-ml pipette. After the tissue was allowed to settle for 5–10 min, the supernatant was collected and the remaining tissue pellet retitrated. The combined supernatants were centrifuged through a 4% bovine serum albumin (BSA) layer and the cell pellet resuspended in neuronal seeding medium, which consisted of B27-Neurobasal Medium (Life Technologies, Carlsbad, CA) supplemented with 1.1% 100× antibiotic-antimycotic solution, 25 μM Na glutamate, 0.5 mM L-glutamine, and 2% B27 Supplement (Life Technologies).

Cell fractionation

Subcellular fractionation was performed as described (Lenferink *et al.*, 2001). Briefly, cell pellets were incubated in a hypotonic buffer (10 mM 4-(2-hydroxyethyl)-1-piperazineethanesulfonic acid, pH 7.2, 10 mM KCl, 1.5 mM $MgCl_2$, 0.1 mM ethylene glycol tetraacetic acid, 20 mM NaF, 100 μM Na_3VO_4, and protease inhibitor mixture) for 30 min at 4°C on a rocking platform. Then cells were homogenized (Dounce, 30 strokes), and their nuclei were pelleted by centrifugation (10 min × 14,000 relative centrifugal force [rcf], 4°C). The supernatant was saved as the cytosolic fraction, and the nuclear pellets were incubated in a nuclear lysis buffer (10 mM Tris-HCl, pH 7.5, 150 mM NaCl, 5 mM EDTA, and 1% Triton X-100) for 1 h at 4°C on a rocking platform. The nuclear fraction was collected by centrifugation (10 min × 14,000 rcf, 4°C).

Western blot analysis

Cells were washed and collected from plates in phosphate-buffered saline (PBS) solution, resuspended with 2× sample buffer, and boiled for 5 min. Proteins were then resolved in 10% SDS–PAGE gel and transferred to a polyvinylidene difluoride membrane (Millipore).

Immunofluorescence analyses

For immunofluorescence analyses, cells were fixed with 4% paraformaldehyde in phosphate buffer, pH 7.4, for 15 min. After washing with 1× PBS, cells were permeabilized with 0.05% Triton X-100 in 1× PBS for 15 min and incubated with preblock buffer (3% BSA, 0.02% Triton X-100 in 1× PBS) for 15 min before being probed with primary antibodies; the following primary antibodies were used: anti-TuJ1 (1:500), anti-SCYL1BP1 (1:250), anti-Mdm2 (1:200), and HA (1:500). All primary antibodies were diluted in preblock buffer and incubated

at 4°C for 18 h. After six washes (six times for 10 min each time) with 1× PBS at room temperature, cells were incubated with secondary antibodies: Alexa 305–anti-goat (1:500), Alexa 488–anti-rabbit (1:500), or Alexa 568–anti-mouse (1:500); all antibodies were diluted in preblock buffer and incubated at room temperature for 1 h, washed with 1× PBS (six times for 10 min each time), and mounted with mounting medium containing Hoechst 33258 (Sigma-Aldrich) to stain nuclei. The immunofluorescence signal was detected by a Nikon confocal microscope (Nikon, Melville, NY).

RNA isolation and RT-PCR analysis

Total RNA was isolated using TRIzol reagent (Invitrogen) and used for RT-PCR analysis. The p53 and Mdm2 probe was made from a cDNA fragment amplified by RT-PCR with an upstream primer (5′-GCC ATC TAC AAG AAG TCA CAA-3′) and a downstream primer (5′-CAG GCA CAA ACA CGA ACC-3′). The Mdm2 probe was made from a cDNA fragment amplified by RT-PCR with an upstream primer (5′-GCG TAA GTG ACC ATT CTG-3′) and a downstream primer (5′-TCT CAC GAA GGG TCC AAC-3′).

Luciferase assay

In all, a luciferase reporter (300 ng) along with pEGFP-N3, SCYL1BP1, BP1-N, or BP1-T (200 ng) and 25 ng of *Renilla* luciferase assay vector pRL-CMV (Promega, Madison, WI) were transfected into PC12 cells plated in a 24-well plate. All experiments were performed in triplicate according to the manufacturer's instructions (Promega).

ChIP assay

ChIP assay was performed according to the manufacturer's instructions (Pierce, Rockford, IL). Briefly, after 2×10^6 PC12 cells or cortical neurons were planted into 100-mm-diameter dishes, chromatin was cross-linked in 1% formaldehyde in PBS, and nuclei were extracted. Chromatin was digested with micrococcal nuclease to yield 500– to 1000–base pair DNA fragments and immunoprecipitated with SCYL1BP1 antibody. After reverse cross-linking and phenol-chloroform extraction, DNA fragments bound by SCYL1BP1 were purified over a column. PCR was performed to visualize the enriched DNA fragments. Primers designed to amplify the Mdm2 promoter were as follows: P1, the 5′-end primer nt −1086 base pairs (CCC CAC TTC CTC CTC GCT CAA) and the 3′-end primer nt −693 base pairs (AGA ACT CGC CAC CGC CCA AC); and P2, the 5′-end primer nt −4 base pairs (GCC AAT GTG CAA TAC CAA CAT GTC) and the 3′-end primer nt +287 base pairs (TGC CTT TCT AAA GCC AGC GTC AG).

Facial nerve transection

Facial nerve transection was performed as described earlier with slight modification (Di Giovanni *et al.*, 2006). Briefly, the animals were anesthetized by an intramuscular injection of a combination of xylazine (13 mg/kg) and ketamine HCl (85 mg/kg). A skin incision was made behind the right ear and the facial nerve exposed; transection was ~2 mm posterior to the foramen stylomastoideum. The wounds were sutured, and the animals were allowed to recover in a dark room on isothermal pads warmed at 37°C for ~30 min.

Recombinant lentiviral vector injection

A week after facial nerve transection, the animals were anesthetized and received lentiviral vector injection into facial nuclei. All injections were made using a 10-µl Hamilton syringe fitted with a glass micropipette (outer diameter, ~60–80 µm) using a Kopf stereotaxic frame (Kopf Instruments, Tujunga, CA). The anteroposterior and mediolateral coordinates were calculated from bregma and the dorsoventral coordinates from the dural surface. Both vector stocks were diluted fivefold in saline before injection. The animals received injections of a total of 3 µl of saline, Lenti-EGFP, or Lenti-EGFP-SCYL1BP1. The injections were made as two 1.5-µl deposits along the needle tract at the following coordinates: anteroposterior, −10.3; mediolateral, −2.0; dorsoventral, −9.5, −8.5. The bregma bar was set at 0.0. The injection rate was 0.25 µl/min, and after the infusion the glass pipette was slowly retracted 1 mm and left in place for an additional 3 min before being withdrawn.

Regeneration in facial nuclei in the brain stem after facial nerve transection was evaluated at day 21 by retrograde axonal tracing with FluoroGold. Three days before being killed, animals from each group were anesthetized, and 1.5 ml of 3% FluoroGold was injected through a micropipette with a tip diameter of 25 mm into the whisker pads bilaterally. After 3 d, the animals were deeply anesthetized and perfused with 0.9% saline solution, followed by 4% paraformaldehyde in 0.1 M phosphate buffer. The brain stem was removed and placed in 30% sucrose for 24 h. The entire facial nuclei were sectioned and reconstructed, and all sections of both facial nuclei per each animal were evaluated (169 for the control and 157 for the transected side). Transverse serial frozen sections, 20 µm thick, were cut and mounted on slides and photographed under a fluorescence microscope. Only labeled neurons with visible nuclei were counted and taken to represent the number of regenerated motor neurons. Thus the overall ratio of FluoroGold-positive neurons was compared in the saline, Lenti-EGFP, and Lenti-EGFP-SCYL1BP1 injection groups (five animals per group). The Abercrombie formula for cell counting was included in our analysis to correct for tissue volume.

Image acquisition and quantitation

Images were obtained using either a Nikon TE2000-S or a Zeiss LSM 510 (Carl Zeiss, Jena, Germany) confocal microscope with 40×/numerical aperture (NA) 1.3 or 63×/NA 1.4 objective. Neuronal morphology was traced and analyzed by Neurolucida software (MBF Bioscience, Williston, VT).

Statistical analysis

Values were expressed as mean ± SEM. Student's *t* test was used to measure significance of differences between two groups. Statistical significance was defined as $p < 0.05$.

ACKNOWLEDGMENTS

We thank Yong Xu and Xingxing Gu for technical aid. This work was supported by the National Basic Research Program of China (973 Program, 2011CB910604 and 2012CB822104); the National Natural Science Foundation of China (31070723, 81070275, 81172879, and 81200828); a project funded by the Priority Academic Program Development of Jiangsu Higher Education Institutions; and the College and University Natural Scientific Research Program of Jiangsu Province (11KJA310002).

REFERENCES

Bernardi R, Scaglioni PP, Bergmann S, Horn HF, Vousden KH, Pandolfi PP (2004). PML regulates p53 stability by sequestering Mdm2 to the nucleolus. Nat Cell Biol 6, 665–672.

Boersma MC, Dresselhaus EC, De Biase LM, Mihalas AB, Bergles DE, Meffert MK (2011). A requirement for nuclear factor-kappaB in developmental and plasticity-associated synaptogenesis. J Neurosci 31, 5414–5425.

Boyd SD, Tsai KY, Jacks T (2000). An intact HDM2 RING-finger domain is required for nuclear exclusion of p53. Nat Cell Biol 2, 563–568.

Di Giovanni S, Knights CD, Rao M, Yakovlev A, Beers J, Catania J, Avantaggiati ML, Faden AI (2006). The tumor suppressor protein p53 is required for neurite outgrowth and axon regeneration. EMBO J 25, 4084–4096.

Di Y *et al*. (2003). Cloning and characterization of a novel gene which encodes a protein interacting with the mitosis-associated kinase-like protein NTKL. J Hum Genet 48, 315–321.
Duan W, Gao L, Wu X, Zhang Y, Otterson GA, Villalona-Calero MA (2006). Differential response between the p53 ubiquitin-protein ligases Pirh2 and MdM2 following DNA damage in human cancer cells. Exp Cell Res 312, 3370–3378.
Fang S, Jensen JP, Ludwig RL, Vousden KH, Weissman AM (2000). Mdm2 is a RING finger-dependent ubiquitin protein ligase for itself and p53. J Biol Chem 275, 8945–8951.
Fuchs SY, Adler V, Buschmann T, Wu X, Ronai Z (1998). Mdm2 association with p53 targets its ubiquitination. Oncogene 17, 2543–2547.
Geyer RK, Yu ZK, Maki CG (2000). The MDM2 RING-finger domain is required to promote p53 nuclear export. Nat Cell Biol 2, 569–573.
Gutierrez H, Davies AM (2011). Regulation of neural process growth, elaboration and structural plasticity by NF-κB. Trends Neurosci 34, 316–325.
Hennies HC *et al*. (2008). Gerodermia osteodysplastica is caused by mutations in SCYL1BP1, a Rab-6 interacting golgin. Nat Genet 40, 1410–1412.
Koh CG (2006–2007). Rho GTPases and their regulators in neuronal functions and development. Neurosignals 15, 228–237.
Kubbutat MH, Vousden KH (1998). Keeping an old friend under control: regulation of p53 stability. Mol Med Today 4, 250–256.
Lenferink AE, Busse D, Flanagan WM, Yakes FM, Arteaga CL (2001). ErbB2/neu kinase modulates cellular p27(Kip1) and cyclin D1 through multiple signaling pathways. Cancer Res 61, 6583–6591.
Leng RP, Lin Y, Ma W, Wu H, Lemmers B, Chung S, Parant JM, Lozano G, Hakem R, Benchimol S (2003). Pirh2, a p53-induced ubiquitin-protein ligase, promotes p53 degradation. Cell 112, 779–791.
Li P (2010). Functional Study on SCYL1 and SCYL1BP1, and Preliminary Research on the Human Protein Interactions between SSX2IP/14-3-3 and ITPKC/PPP3CC, PhD Thesis. Shanghai, China: Fudan University, 43–48.
Logan IR, Sapountzi V, Gaughan L, Neal DE, Robson CN (2004). Control of human PIRH2 protein stability: involvement of TIP60 and the proteosome. J Biol Chem 279, 11696–11704.
Ma X, Fei E, Fu C, Ren H, Wang G (2011). Dysbindin-1, a schizophrenia-related protein, facilitates neurite outgrowth by promoting the transcriptional activity of p53. Mol Psychiatry 16, 1105–1116.
Maki CG, Huibregtse JM, Howley PM (1996). In vivo ubiquitination and proteasome-mediated degradation of p53(1). Cancer Res 56, 2649–2654.
Marine JC, Francoz S, Maetens M, Wahl G, Toledo F, Lozano G (2006). Keeping p53 in check: essential and synergistic functions of Mdm2 and Mdm4. Cell Death Differ 13, 927–934.
Miller FD, Kaplan DR (2003). Signaling mechanisms underlying dendrite formation. Curr Opin Neurobiol 13, 391–398.
Prives C (1998). Signaling to p53: breaking the MDM2-p53 circuit. Cell 95, 5–8.
Qin Q, Baudry M, Liao G, Noniyev A, Galeano J, Bi X (2009). A novel function for p53: regulation of growth cone motility through interaction with Rho kinase. J Neurosci 29, 5183–5192.
Qin Q, Liao G, Baudry M, Bi X (2010). Role of calpain-mediated p53 truncation in semaphorin 3A-induced axonal growth regulation. Proc Natl Acad Sci USA 107, 13883–13887.
Raivich G *et al*. (2004). The AP-1 transcription factor c-Jun is required for efficient axonal regeneration. Neuron 43, 57–67.
Tedeschi A, Nguyen T, Puttagunta R, Gaub P, Di Giovanni S (2009a). A p53-CBP/p300 transcription module is required for GAP-43 expression, axon outgrowth, and regeneration. Cell Death Differ 16, 543–554.
Tedeschi A, Nguyen T, Steele SU, Feil S, Naumann U, Feil R, Di Giovanni S (2009b). The tumor suppressor p53 transcriptionally regulates cGKI expression during neuronal maturation and is required for cGMP-dependent growth cone collapse. J Neurosci 29, 15155–15160.
Whitford KL, Dijkhuizen P, Polleux F, Ghosh A (2002). Molecular control of cortical dendrite development. Annu Rev Neurosci 25, 127–149.
Yan J, Di Y, Shi H, Rao H, Huo K (2010a). Overexpression of SCYL1-BP1 stabilizes functional p53 by suppressing MDM2-mediated ubiquitination. FEBS Lett 584, 4319–4324.
Yan J, Zhang D, Di Y, Shi H, Rao H, Huo K (2010b). A newly identified Pirh2 substrate SCYL1-BP1 can bind to MDM2 and accelerate MDM2 self-ubiquitination. FEBS Lett 584, 3275–3278.
Zhang J, Yan W, Chen X (2006). p53 is required for nerve growth factor-mediated differentiation of PC12 cells via regulation of TrkA levels. Cell Death Differ 13, 2118–2128.
Zhang L, Li J, Wang C, Ma Y, Huo K (2005). A new human gene hNTKL-BP1 interacts with hPirh2. Biochem Biophys Res Commun 330, 293–297.